Wave function of ^{14}N

K. Amos, D. Koetsier, and D. Kurath*
School of Physics, The University of Melbourne, Parkville, Victoria, 3052 Australia
(Received 16 January 1989)

The β- and γ-decay rates, electron scattering form factors, and intermediate energy (p,p') and $(\mathbf{p},n)$ cross-section data are used to compare a set of wave functions that have been proposed for ^{14}N. With pertinent reaction t matrices and allowance for reasonable and often small core polarization corrections the wave functions derived by standard (shell-model) calculations are found to be the most relevant.

I. INTRODUCTION

Intermediate energy nucleon inelastic and charge exchange reactions upon mass 14 nuclei provide an interesting data base with which to study elements of conventional distored wave approximation (DWA) analyses. Transitions amongst the low lying states isolate most individual components of spin and isospin transfer; with some being particularly sensitive to the individual components (central, spin-orbit, tensor) of the two nucleon transition t matrices. Furthermore $0p$ shell-model calculations are available[1] from which many of the known static and dynamic properties of the low lying spectra are well reproduced. These structure calculations have the particularly useful property that the transition density matrices are readily expressed in either j-j or L-S coupling form with a simple transformation relating the two schemes. Also, with either convention, those transition density matrix elements are few in number. Indeed, these features were essential for recent studies[2,3] of the ground and 0^+ $T=1$ (2.313 MeV) states of ^{14}N. Therein static moments and electron scattering form factors were used to determine the $0p$ shell-model wave functions without recourse to any starting Hamiltonian. However, the wave functions so deduced are not eigenfunctions of any Hamiltonian one may deem reasonable for mass 14 nuclei. The problem it appears is that the limitations of the $0p$ shell basis space vary with the state of the system considered.

It has long been known that higher shell and/or multi-$\hbar\omega$ excitations are (core polarization) corrections that can alter $0p$ shell-model transition probabilities by large factors.[4] For weak transitions such factors can be orders of magnitude. Typically, however, to compare with data, $0p$ shell-model estimates of β-decay rates need be quenched by values in the range 0.8–0.9, as is usually also the case for calculated magnetic multipole γ-decay rates, while it is common that measured $E2$ γ-decay rates are twice those calculated. Thus one anticipates a need to vary the $0p$ shell-model transition densities to fit other (scattering) data as well. Such variations, however, must be consistent for all complementary data. Thus the conventional approach to use of shell-model structure in data analyses is to start with a proper (limited) basis model of structure and then allow variation of the transition density matrix elements given under the constraint that electromagnetic and hadronic transition data are all fit. The variations are then identified as core polarization corrections. To do so, however, one must have a good specification for each and every reaction t matrix. Such was the case in a study[5] of the excitation of the 2_1^+ (4.44 Me) state in ^{12}C for which transition density matrix elements from both $0p$ shell and large basis projected Hartree-Fock models were available. Thereby a direct correlation was possible between the core polarization variation of the $0p$ shell-model transition densities and the higher shell components as specified by the projected Hartree-Fock method.

But core polarization corrections can be, and are,[6] momentum transfer dependent. Thus it may be that scale values on transition density matrices to match $0p$ shell-model calculations results to zero momentum transfer data such as β- and γ-decay rates differ from those required to have calculated form factors (at finite momentum transfer) match observation. Even so, the conventional method must still show consistency with data at appropriate momentum transfer values. Such was demonstrated in a recent study[7] of select transitions in ^{13}C(^{13}N) and of the available β- and γ-decay rates, electron scattering form factors, and (p,p') and (p,n) cross sections taken with intermediate energy protons. We consider herein the ^{14}N(^{14}C) case.

A discussion of the structure of ^{14}N with a critique of the wave functions specified by Huffmann *et al.*[3] is given in the next section. Therein, the available electromagnetic properties and transitions are discussed. The inelastic proton scattering and charge exchange data and our analyses of them are discussed in Sec. III.

II. THE WAVE FUNCTIONS OF ^{14}N

There are many model wave functions for ^{14}N proposed in the literature but they can be classified broadly into two classes. The first class contains those determined by specifying a Hamiltonian for light nuclei and tuning it to be reproduce the observed spectra and static moments. The Cohen and Kurath[1] wave functions and their subsequent variations are examples of this class of model wave function. Herein we will consider two such *C-K* model calculations of wave functions identifying

each by the matrix elements (8-16) *POT* and (8-16) 2*BME* that define the specific Hamiltonian. The second class of wave functions are determined by selecting a general, parametrized form for the wave functions and determining the strength coefficients, subject to a normalization constraint, by fitting a select set of static and dynamic observables. The set of coefficients so determined by Ensslin *et al.*[2] as well as the sets identified as *H*1, *H*2, and *HF*1 in the study by Huffmann *et al.*,[3] are examples which we consider herein. The precept upon which this latter class of function is based is that all selected data can be understood with nuclear structure limited to the 0*p* shell. A useful consequence is that there are few wave function components to each state and concommitantly few transition density matrix elements. Huffmann *et al.*[3] used the static magnetic moment of ^{14}N, the radiative lifetime of the 2.313 MeV 0^+ $T=1$ state, the ^{14}C (β^-) ^{14}N Gamow-Teller matrix element, and the electron scattering transverse form factors to determine their wave functions finding that the best, the *HF*1, has the 2.313 MeV state very close to the L-S coupling limit.

Given that ^{14}C is the isobaric analogue of the 2.313 MeV state in ^{14}N, the electromagnetic transition in ^{14}C leading to the 1^+ $T=1$ state at 11.31 MeV is of particular interest. In a representation of mass 14 states as two holes (coupled) in ^{16}O, the 11.31 MeV state is of purely $^3P_1$ classification, and so its $M1$ excitation from the ground directly reflects the degree of $^3P_0$ in the mix (with $^1S_0$) that is the ^{14}C ground state, and by inference in the isobaric analogue at 2.313 MeV in ^{14}N. The various model wave functions can be recast in the coupled two hole form and the associated amplitudes are as listed in Table I. From this tabulation, it is clear that the *C-K* 0^+ $T=1$ wave functions are different from all of the fitted ones. The Ennslin and H1 states are almost pure $^3P_0$ while the H2 and HF1 states are almost pure $^1S_0$ in character. One may likewise decompose the ground state of ^{14}N into $^3S_1$, $^3D_1$, and $^1P_1$ components. The models all vary in their mix of these functions although the *C-K* mix of $^3D_1$ and $^1P_1$ are very much like that of the "best fitted" HF1 wave function. But it is the $^3P_0$ character of the 0^+ $T=1$ state that is of immediate concern, since the $B(M1)$ value as measured by Crannell *et al.*[8] for the excitation of 11.31 MeV isovector 1^+ state in ^{14}C is 1.23 ± 0.25 μ_N^2. A pure $^1S_0$ ground state would have a zero probability for the $M1$ excitation. To estimate this $B(M1)$ value using the various model wave functions, we need the transition density matrix elements that are defined by

TABLE I. Two-nucleon hole components of the 0^+ $T=1$ wave functions.

Model	$^1S_0$	$^3P_0$
(8-16) *POT*	0.859	0.512
(8-16) 2*BME*	0.847	0.532
Ensslin	−0.093	0.996
H1	−0.361	0.932
H2	1.000	−0.002
HF1	0.999	−0.062

$$A_{1(\mathrm{L,S})}=\sum_{j_1 j_2}[(2j_1+1)(2j_2+1)(2L+1)(2S+1)]^{1/2}\begin{Bmatrix}1 & \frac{1}{2} & j_1\\ 1 & \frac{1}{2} & j_2\\ \mathrm{L} & \mathrm{S} & 1\end{Bmatrix}\langle {}^{14}C;1^+1\|[a^\dagger_{j_2}xa_{j_1}]\|{}^{14}C;0^+1\rangle \tag{1}$$

In the LS component representation with C_S, C_P being the amplitudes of the S and P state admixtures in the ^{14}C ground state these transition density matrix elements have the values

$$\begin{aligned}A_{1(21)}&=\sqrt{5}C_P/6\ ,\\ A_{1(11)}&=\sqrt{3}C_P/6+\sqrt{2/3}C_S\ ,\\ A_{1(01)}&=2C_P/3\ ,\\ A_{1(10)}&=-\sqrt{6}C_P/6\ ,\end{aligned} \tag{2}$$

and from which the $B(M1)$ for excitation of the 11.31 MeV (pure $^3P_1$) isovector 1^+ state is

$$B(M1\uparrow)=\frac{6}{\pi}(\mu_P-\tfrac{1}{2})^2C_P^2$$

The $A_{1(\mathrm{LS})}$ values for the various wave functions are given in Table II and the $B(M1)$ estimates are listed in the last column of that table. Of these the *C-K* wave functions are closest to the empirical value; being twice the observed transition probability. The *C-K* wave functions are thus the only ones of this set that can reproduce the experimental results with but a reasonable amount of core polarization. It will be of considerable interest to measure inelastic scattering form factors if that be feasible with a ^{14}C target.

The foregoing is not the only reason to be concerned about the fitted wave functions. The amplitude ratio,

$$C(^1S_0)/C(^3P_0)\equiv\beta\ , \tag{3}$$

is a measure of the 0*p* shell matrix elements of the Hamiltonian. The two-body interaction potential leads to

$$\begin{aligned}v_S&\equiv\langle {}^1S_0|v|{}^1S_0\rangle\ ,\\ v_P&\equiv\langle {}^3P_0|v|{}^3P_0\rangle\ ,\\ v_{SP}&\equiv\langle {}^3P_0|v|{}^1S_0\rangle\ ,\end{aligned} \tag{4}$$

TABLE II. Transition density matrix elements $A_{1(L,S)}$ from the excitation of the isovector 1^+ state at 11.31 MeV in ^{14}C.

Model	$A_{J(L,S)}$ 1(2,1)	1(1,1)	1(1,0)	1(0,1)	$B(M1)$ $(\mu_N)^2$
8-16 *POT*	0.191	0.849	−0.209	0.342	2.634
8-16 *2BME*	0.198	0.845	−0.217	0.355	2.842
Ensslin	0.371	0.212	−0.407	0.664	9.955
H1	0.347	−0.026	−0.380	0.621	8.714
H2	−0.0007	0.816	0.0008	−0.0013	4×10^{-5}
HF1	−0.023	0.797	0.025	−0.041	0.038

for the two holes in ^{16}O. Since the $^1S_0$ and $^3P_0$ wave functions have opposite spatial symmetry, one would usually have $v_{SP}=0$ as in the (8-16) *POT* case. However, in obtaining an effective interaction in a truncated space such as the $(0p)$ shell, a nonzero value of v_{SP} is possible. This freedom was allowed in the (8-16) *2BME* fit to energies which resulted in the value $v_{SP}=-0.24$ MeV (a small value). In addition to the v contributions there is the single hole contribution ϵ_3 for a $0p_{3/2}$ hole and ϵ_1 for a $0p_{1/2}$ hole. As suggested by Talmi,[9] the resultant (2×2) eigenvalue problem can be used to assess the wave functions for the lowest λ eigenvalue:

$$\begin{vmatrix} V_s+\frac{4}{3}\epsilon_3+\frac{2}{3}\epsilon_1-\lambda, & V_{SP}-\sqrt{8/9}(\epsilon_3-\epsilon_1) \\ V_{SP}-\sqrt{8/9}(\epsilon_3-\epsilon_1), & V_P+\frac{2}{3}\epsilon_3+\frac{4}{3}\epsilon_1-\lambda \end{vmatrix}=0 . \quad (5)$$

For the lower eigenvalue, the ratio β of Eq. (3) must have a sign opposite to that of the off diagonal matrix element, i.e.,

$$\beta/|\beta|=-(v_{SP}-\sqrt{8/9}\epsilon)/|v_{SP}-\sqrt{8/9}\epsilon| . \quad (6)$$

From ^{15}N we know that single-hole splitting for a $(0p)$ model is

$$\epsilon\equiv\epsilon_3-\epsilon_1=6.3 \text{ MeV} . \quad (7)$$

For the lower four wave functions of Table I, β is negative, so that Eq. (5) requires

$$\begin{aligned} &v_{SP}-\sqrt{8/9}\epsilon>0 , \\ &v_{SP}>5.94 \text{ MeV} . \end{aligned} \quad (8)$$

Such a large value of a symmetry violating matrix element is unreasonable and so we must reject the fitted wave functions as viable candidates for the low excitation mass 14 wave functions. If so, the circumstances and data that encouraged others to look beyond the *C-K* wave functions must be reappraised.

A composite set of transition probabilities, of both β and γ decay of select low lying states in mass 14 nuclei[8] is given in Table III. Therein the experimental values are compared with the results calculated using the (8-16) *POT* and (8-16) *2MBE* shell-model structure models. When required, the standard length of 1.64 fm for the harmonic oscillator, single nucleon wave functions was used. The β^- and β^+ decay probabilities from ^{14}C and ^{14}O and to the ground state and 3.95 MeV states in ^{14}N, respectively, compare favorably with the Cohen and Kurath calculated values. It must be remembered that the β^- decay of ^{14}C is unusually weak, and it has been noted[4] that small *s-d* shell admixtures can reduce the (small) Cohen and Kurath value to zero. The analogue (^{14}O) state decays by β^+ emission to the ground, 2.313 and 3.95 MeV state in ^{14}N of which the analogue state transition (to the 2.313 MeV in ^{14}N) is very predominant. Nevertheless, the decay to the 3.95 MeV state is sufficient to give the transition probability specified in Table III.

Three $B(M1)$ decay values are listed next in Table III with the first two associated with the dipole transitions in ^{14}C and ^{14}N, respectively. The ^{14}C transition has a reasonable strength and, and as is usual with limited based calculations, the shell-model estimates are too large. Indeed, a reduction by a factor of 2 is quite typical. The 2.313 MeV isovector transition in ^{14}N is unusu-

TABLE III. $0p$-shell model values of β- and γ-decay rates.

Measured transition	Experimental value	*C-K* (8-16) *POT*	*C-K* (8-16) *2BME*
β-decay B_{GT} values			
^{14}C$(\beta^-)^{14}$N1^+0 (g.s)			
^{14}O$(\beta^+)^{14}$N$1^+0(3.95)$	3.24±0.45	4.81	
$B(M1)\downarrow$values (μ_N^2)			
^{14}C: $1^+1\rightarrow0^+1(11.31)$	(0.41±0.08)	0.829	0.937
^{14}N: $0^+1\rightarrow1^+0(2.313)$	$(5.05\pm0.11)10^{-2}$	3.96×10^{-2}	3.34×10^{-2}
^{14}N: $1^+0\rightarrow1^+0(3.95)$	$(5.7\pm1.7)\times10^{-4}$	1.52×10^{-3}	3.34×10^{-5}
$B(E2)\downarrow$values $(e^2$ fm$^4)$			
^{14}N: $1^+0\rightarrow1^+0(3.95)$	3.6 ±0.3	1.761	1.561

ally weak and it is not surprising that the shell-model estimates then are comparable and even a little weaker than the measured value. Likewise, the isoscalar $B(M1)$ value for the excitation from ground of the 3.95 MeV state is very small and, in this instance, the two Cohen and Kurath calculated results lie either side of the empirical one. On the other hand, the $B(E2)$ value for the (isoscalar) excitation of the 3.95 MeV state is two to three times the shell-model estimates. Such is consistent with a polarization charge of $0.3e$; a value that is quite acceptable as a measure of the expected core polarization corrections to limited basis shell-model calculations.

The recent measurement[3] of transverse electron scattering form factors with which a set of fitted wave functions were defined, also were analyzed therein using the (8-16) *POT* and (8-16) *2BME* wave functions to compute both the ground-state (elastic) and 0^+ $T=1$ excitation $M1$ form factors. Those calculated ground-state form factors were in excellent agreement with the data to 2 fm^{-1} but exceeded the maximum in the inelastic scattering form factor data by a factor of 2 to 3 in contradistinction to the (weak) $B(M1)$ values. But the finite q, electron scattering form factor is dominated by contributions weighted by the J(L,S) amplitude $A_{1(2,1)}$. Other, finite q transition data are needed to confirm the degree of quenching of this $0p$ shell-model component. Such is provided by analyses of intermediate energy (p,p') data and this we discuss in the next section.

III. HADRON SCATTERING DATA ANALYSES

We report the results of DWA analyses of inelastic and charge exchange scattering of protons from ^{14}C (^{14}N). The calculations were made using a upgraded version of the code[10] DWBA70 in which density and energy dependent two-nucleon t matrices[11] can be used. Analyses have been made of 122 MeV data[12] and of 160 MeV data[13,14] and we have used the optical model potentials specified in those studies. We have also used harmonic oscillator single particle wave functions with an oscillator length of 1.64 fm as deemed most pertinent from the analyses of the electron scattering form factors.

The differential cross sections from the excitation of the 0^+ $T=1$ state at 2.313 MeV in ^{14}N are displayed in Figs. 1 and 2 with the (160 MeV) analyzing power values given in Fig. 3. As part of the 160 MeV differential cross-section data we include the appropriately scaled, 160 MeV (p,n) cross sections obtained from ^{14}C and leading to the ground state of ^{14}N. This charge exchange reaction involves the same matrix elements in DWA analyses as does the (p,p') transition to the 0^+ $T=1$ state in ^{14}N when it is assumed that the ^{14}C ground state is its isobaric analogue.

This isovector dipole transition involves $L=0$ and $L=2$ component matrix elements and the result of any calculation is very sensitive to the interference between them. Concommitantly, calculated results are very sensitive not only to details of the two-nucleon t matrices but also to specifics of the chosen models of nuclear structure (transition density matrix elements). This sensitivity to choice of t matrix and model of nuclear structure is

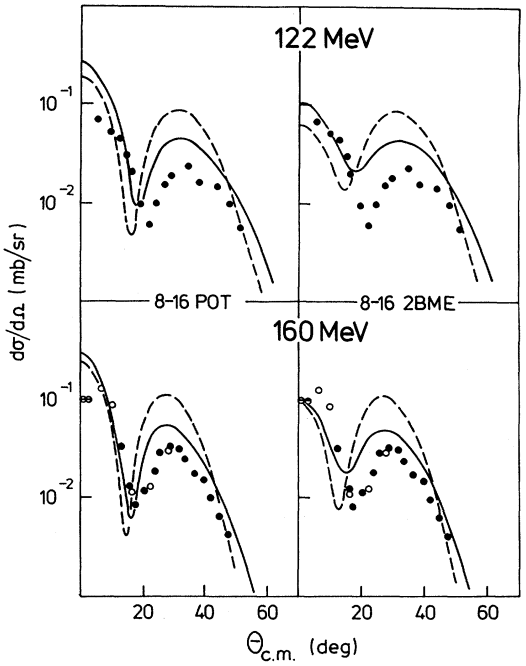

FIG. 1. The differential cross sections from the excitation of the 0^+ $T=1$ state at 2.313 MeV in ^{14}N by inelastic proton scattering. The open circles are the data taken by the complementary study of the ^{14}C(p,n) reaction to the ground state of ^{14}N.

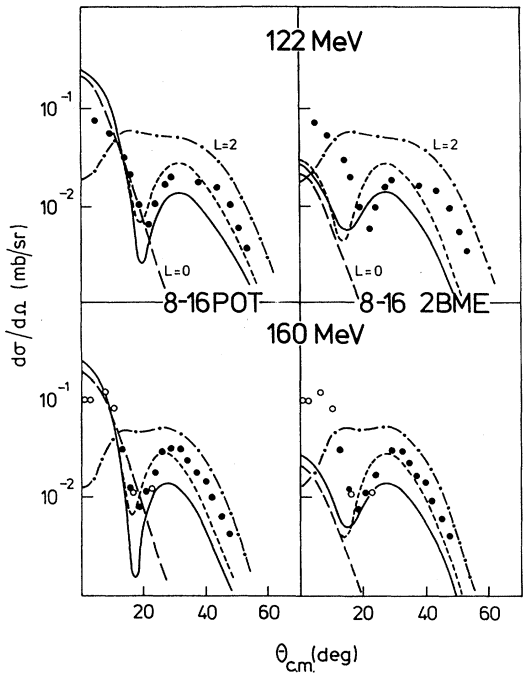

FIG. 2. Same as Fig. 1 but with component results from our DWA calculations as described in the text.

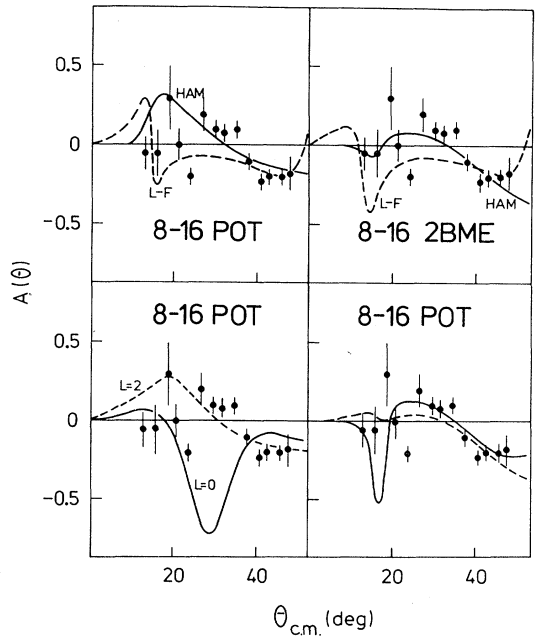

FIG. 3. The analyzing power data from the inelastic scattering of 160 MeV (polarized) protons to the 2.313 MeV 0^+ $T=1$ state in ^{14}N.

shown in Fig. 1. Therein the 122 MeV data[12] (top) and 160 MeV data[13,14] (bottom) are compared with the results of DWA calculations made using the Hamburg density dependent and *L-F* effective *t* matrices.[15] These Hamburg *t*-matrix results are displayed by the solid curves while those obtained using the *L-F t* matrix are shown by the dashed curves. The two Cohen and Kurath models of structure,[1] i.e., those made using the (8-16) *POT* and (8-16) *2BME* matrix elements, were used to obtain the results displayed on the left and right sides of Fig. 1, respectively.

The differences obtained when the Hamburg and *L-F t* matrices are used are most noticeable. With either model of spectroscopy, use of the *L-F t* matrices in calculations gives more sharply varying cross sections than are obtained from those made using the Hamburg *t* matrices. The second maxima in the 20–40° region is twice as strong and the minima occur at smaller values of momentum transfer. These differences do not reflect density dependence of the *t* matrices. Indeed if the density dependences of the Hamburg (isovector) *t* matrices are ignored—so that the "free" two-nucleon. Hamburg *t* matrices are used—the results are little different to those given. It has been noted before[16] that density dependence effects are essentially isoscalar in character.

Overall, use of the Hamburg *t* matrices and the (8-16) *POT* model nuclear transition density matrix elements give the best results. But these cross sections are the result of significant interference between $L=0$ and $L=2$ multipole matrix elements. This interference is due primarily to the central and tensor attributes of the two-nucleon *t* matrices, but both direct and exchange (knockout) contributions are important as well.

The $L=0$ and $L=2$ multipole contributions to the calculations made using the Hamburg *t* matrices and with the two *C-K* models of spectroscopy are displayed by the long dash and dash-dot curves in Fig. 2. Their matrix elements add coherently to yield the solid curve results shown in Fig. 1, although beyond 30°, the results are almost pure $L=2$ in nature. The electron scattering form factors have been fit by reducing the spectroscopic amplitudes $A_{J(\mathrm{L,S})}$ for J(L,S) of 1(2,1) by a half (a factor of 4 in the form factor therefore) and if such is also done in the (p,p') calculations then the solid curves given in Fig. 2 are the result. But there is also evidence[7,17] that the isovector tensor components in the Hamburg *t* matrices are too weak. If, in addition then, the isovector tensor force is increased by 40% in strength, calculations give values depicted by the small dash curves. The resultant (8-16) *POT* model calculated cross sections are then in very good agreement with the data over most of the measured range of scattering angles. Of the details not fit by these optimal calculations, the position of the minimum and the very small angle data are the most evident. More realistic single-particle wave functions than those used herein may alter the calculated results (as has been observed recently[17] for transitions to stretched, unnatural parity states) but the small angle ($<25°$) variations in this transition are most strongly influenced by the many nucleon structure of the states per the transition density matrix elements. We note that the essential difference between the two *C-K* models is the value of the 1(0,1) spectroscopic amplitude, for which the (8-16) *POT* value is three times larger than that of the (8-16) *2BME* structure calculation. It is no surprise therefore to find 0° cross sections by using these two models of structure that differ by almost an order of magnitude. In this case one cannot use the associated β-decay rate to make a selection as it is a very weak transition and small core polarization effects drastically alter calculated values. Such small core polarization corrections are negligible in effect for proton induced reactions at small momentum transfer. Rather the small angle variation is sensitive to the chosen 0*p* shell-model structure and also to the component structure of the two-nucleon *t* matrix. The central force dominates the $L=0$ matrix elements while it is the tensor force that gives the most significant $L=2$ values. Even at 0° scattering the tensor force gives a finite $L=2$ value which can be comparable to that of the $L=0$ matrix element dependent upon the chosen model of structure. Thus extraction of the β-decay matrix element from the (p,n) cross section at 0° for such a sensitive transition is mot problematic.

The analyzing power is more sensitive to matrix element details than is the differential cross section. The data[14] and DWA results for the analyzing power from the inelastic scattering of 160 MeV protons to the 0^+1 state in ^{14}N are presented in Fig. 3. In the top panels the solid and dashed curves display the results obtained using the Hamburg and *L-F t* matrices, respectively, with the (8-16) *POT* and (8-16) *2MBE* models of structure as indicated. The *L*-component contributions to the calculations made using the Hamburg *t* matrix and (8-16) *POT* transition density matrix elements are displayed in the bottom left hand portion of this figure. In the remaining

part of this figure we show the calculated results obtained by using the (8-16) *POT* model of nuclear structure but with the 1(2,1) transition density matrix element scaled to a fit to the electron scattering form factor. Using the Hamburg t matrix the result is that shown by the solid curve while the dashed curve depicts the result obtained with the Hamburg t matrix but with its isovector tensor strength enhanced by 40%.

The data above 30° scattering reflect the $L=2$ component for all calculations but at angles forward of this the $L=0$ and $L=2$ interference effects are marked. Of all the results shown, those depicted by the dashed curve in the bottom right-hand diagram are the most significant not only as they are the results obtained from use of spectroscopy tuned to fit the electron scattering form factor and with the "optimal" t matrix, but also as the differential cross section is reasonably well fit. Without a fit to the differential cross section any match to the analyzing power data is at best fortuitous. We note that our results are better than those obtained by using any of the fitted (to the electron scattering form factor) 0p shell wave functions; albeit that the (p,p') calculation results reported therein[3] were obtained using the *L-F t* matrices.

Core polarization corrections to structure are known to alter calculation magnitudes and also they should be momentum transfer dependent.[4-6] For the isovector dipole (^{14}N) transition, Rose, Häusser, and Warburton[4] have shown that a small amount of *s-d* shell admixing that is due to the tensor force (in structure calculations) can explain the variation from the *C-K* models estimates of measured γ-decay rates and β-decay rates and for this isovector dipole transition in particular. Notably, the strongly inhibited Gamow-Teller matrix element for the β decay of ^{14}C can be made vanishingly small. On the other hand, the $M1$ (γ-decay) matrix element receives constructive interference from small (8%) *s-d* shell admixtures to the 0p shell model and the result is then in better agreement with the measured value. Such *s-d* shell admixtures, however, have little influence in finite momentum transfer calculations such as those of the transverse electron scattering form factor and inelastic scattering cross sections.

In Fig. 4, the differential cross sections from 122 and 160 MeV proton inelastic scattering and the analyzing power at 160 MeV excitation of the 1^+ $T=0$ state 3.95 MeV in ^{14}N are compared with the results of our DWA calculations. The (8-16) *POT* wave functions were used to specify the basic transition density matrix elements required in these calculations. The results displayed in the left hand panel were obtained using the Hamburg t matrices (solid curves) and the *L-F t* matrices (dashed curve). Both are reasonable fits to the data with now the cross section showing the typical density dependence signature[5] of reduced (from cross-section values calculated using the free t matrix) small angle cross sections and a "shoulder" effect at higher momentum transfer values.

This isoscalar transition is dominated by the $L=2$ multipole contributions. Such is evident from the component results underlying the (modified) Hamburg calculated values displayed by the solid curves in the right-hand panel of Fig. 4. In those calculations the 2(2,0) spectroscopic amplitudes have been enhanced by 1.37; a value which brings the calculated $B(E2)$ for the γ-decay of this 1^+ $T=0$ state into agreement with observation. Evidently that enhancement is too large unless the spin 1 transfer contributions can also be varied to compensate. However, there is no independent experimental measure of this 2(2,1) strength to date.

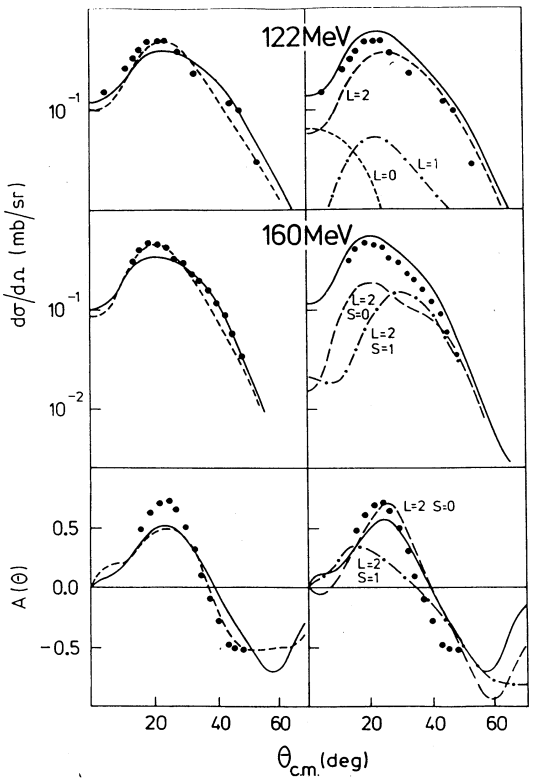

FIG. 4. The differential cross sections and analyzing powers from the inelastic scattering of protons to the isoscalar 1^+ state at 3.95 MeV in ^{14}N.

The 122 MeV calculations (top right-hand panel) display the complete $L=2$ ($S=0$ plus $S=1$), $L=1$, and $L=0$ contributions while the separate spin 0 and spin 1 transfer $L=2$ multipole contributions are shown for the 160 MeV calculations (middle and bottom right-hand diagrams). Clearly, the $L=2$ contributions dominate but now, and unlike the quadrupole excitation of the 4.4 MeV state in ^{12}C, the spin transfer contributions are comparable to those of zero spin transfer.

Finally, in Fig. 5, we present a comparison of our calculated DWA results with the data from the charge exchange, 160 MeV scattering from ^{14}C and leading to the 1^+ $T=0$ state at 3.95 MeV in ^{14}N. This isovector dipole transition is dominated by the $L=0$, $S=1$ transition density matrix. Furthermore the central force attributes of the t matrices give the largest scattering amplitudes in the calculations although the contributions of the tensor force are not insignificant. The differential cross section and analyzing power data are compared with the DWA calculations made using the (8-16) *POT* set of transition

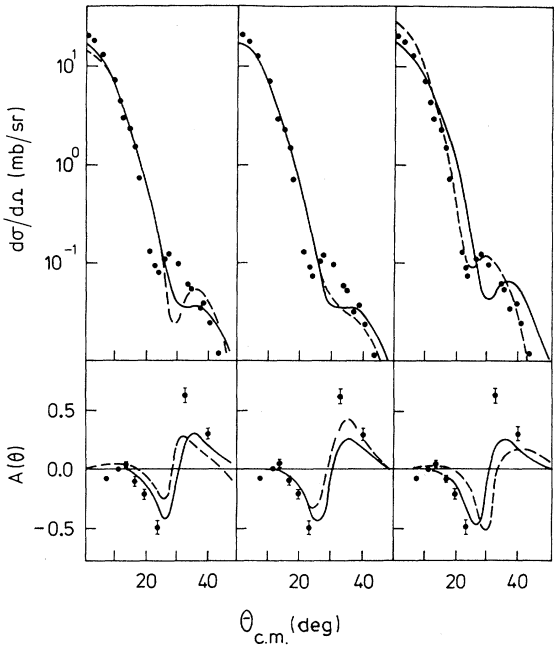

FIG. 5. The differential cross sections and analyzing powers from the $^{14}C(p,n)$ transition to the 3.95 MeV 1^+ $T=0$ state in ^{14}N.

densities and the Hamburg (solid) and *L-F* (dash) t matrices in the left-hand panel. DWA calculations made using the Hamburg t matrix and the (8-16) *POT* (solid) or (8-16) *2BME* (dash) transition density matrix elements are given in the central panel. In the remaining panel are shown the results of a DWA calculation made using the (8-16) *POT* structure model and the Hamburg t matrix modified by enhancing the isovector tensor force by 40% (solid curve). It is compared therein with the result of a previous calculation[14] in which an oscillator length of 2.0 fm was used. Clearly there is little to choose between the results obtained with any calculation made with sensible oscillator parameter values. All give a reasonable representation of the main feature of the data. The enhancement of the isovector tensor force component in the Hamburg t matrix gives a second, minor, maximum in the cross section but at a higher momentum transfer value of that observed.

IV. CONCLUSIONS

The standard $0p$ shell-model wave functions are quite good first estimates of the structure of and transitions between low excitation states in ^{14}N. Our analyses of the (p,p') cross sections, and the complementary ^{14}C (p,n) transition data, have shown that calculated results involve destructive interference for some (low) values of momentum transfer. Thus small angle predictions are very sensitive to details of both nuclear structure and reaction mechanism. Indeed, using the Hamburg density dependent t matrices with an enhanced (by 40%) isovector tensor force and transitions density matrices given by the (8-16) *POT* $0p$ shell-model wave functions adjusted to fit the transverse form factors from electron scattering, the hadron scattering cross sections and analyzing power data are well fitted. Esoteric wave functions as proposed by the recent analysis of Huffman *et al.*[3] are not required.

Specifically, the isovector dipole transitions, $1^+0\rightarrow 0^+1$ (2.313 MeV) for ^{14}N (p,p') and the $0^+1\rightarrow 1^+0$ ^{14}C (p,n) ^{14}N (ground state), confirm the need to reduce the transition densities $A_{1(2,1)}$ by one half as is assessed from the fit to the electron scattering form factor. Furthermore, at zero momentum transfer, the dominant $L=0$ transition strength can change by an order of magnitude with realistic variation of wave functions. With increasing (small q), these $L=0$ (central force) and $L=2$ (tensor force) amplitudes interfere markedly. The hadron scattering data in this small momentum region clearly indicates a preference for the (8-16) *POT* wave functions. It appears that the anomalously weak β decay of ^{14}C to the ground state of ^{14}N is then the result of further (destructive) interference of higher shell (core polarization) contributions to the transitions as suggested by Rose, Häusser, and Warburton.[4] With the amounts required to give vanishing β-decay rates from the (8-16) *POT* spectroscopy, the electron form factors and hadron cross sections are but little affected. Likewise, the density dependence of the t matrix causes no major effect in the momentum transfer dependence of cross-section results. But the component character strengths and ranges of the pertinent t matrix are crucial in giving results not only in agreement with data but also consistent with a fit to the electron scattering form factor. The other isovector dipole transition considered, $^{14}C(p,n)$ to the 1^+ $T=0$ state at 3.95 MeV in ^{14}N, is dominated by central force effects and again results are little influenced by any density dependence of the t matrix. Both $0p$ shell models of spectroscopy give a reasonable fit to this data and each must be quenched with weights consistent with that required to match the observed, relevant, β-decay probability.

The (isoscalar) inelastic scattering excitation of the 1^+ $T=0$ state at 3.95 MeV in ^{14}N is dominated by the $L=2$ components of the transition densities. Unlike the comparison transition, $0^+\rightarrow 2^+$ (4.44 MeV) in ^{12}C, the J(L,S) contributions from the 2(2,0) and 2(2,1) aspects of the ^{14}N spectroscopy are comparable. A simple enhancement of the 2(2,0) amplitudes to give the measured $B(E2)$ for γ decay gave a slightly better fit to data shape but the (p,p') cross sections are too large. Some appreciable reduction of the 2(2,1) transition density matrix element is then required to fit the data. It is of interest to obtain other data, such as the transverse electron scattering form factor, to corroborate this suggestion. Finally we note that, for this transition, the density dependence of the t matrix is important. The data display the associated, characteristic momentum transfer variations of the isoscalar quadrupolar transitions.[5]

ACKNOWLEDGMENTS

We wish to thank Professor I. Talmi for his suggestions on handling of the nuclear structure calculations. One of us (D.K.) also wishes to thank the University of Melbourne for its hospitality during his sabbatical.

*On leave from the Argonne National Laboratory, Argonne, IL 60439.

[1]S. Cohen and D. Kurath, Nucl. Phys. **73**, 1 (1965); **A101**, 1 (1967); T.-S. H. Lee and D. Kurath, Phys. Rev. C **21**, 293 (1980).

[2]N. Ensslin, W. Bertozzi, S. Kowalski, C. P. Sargent, W. Turchinetz, C. F. Williamson, S. Fivozinsky, H. Lightbody, and S. Penner, Phys. Rev. C **9**, 1704 (1974); N. Ensslin, Ph.D. dissertation, Massachusetts Institute of Technology, 1972.

[3]R. L. Huffman, J. Dubach, R. S. Hicks, and M. A. Plum, Phys. Rev. C **35**, 1 (1987).

[4]H. J. Rose, O. Häusser, and E. K. Warburton, Rev. Mod. Phys. **40**, 591 (1968).

[5]K. Amos and I. Morrison, Phys. Rev. C **19**, 2108 (1979); W. Bauhoff, S. F. Collins, R. S. Henderson, G. G. Shute, B. M. Spicer, V. C. Officer, K. A. Amos, I. Morrison, D. W. Devins, D. L. Friesel, and W. P. Jones, Nucl. Phys. **A413**, 255 (1984).

[6]K. Amos and L. Berge, Phys. Lett. **127B**, 299 (1983); K. Amos, L. Berge, and R. de Swiniarski, Nucl. Phys. **A485**, 653 (1988).

[7]K. Amos, L. Berge, and D. Kurath, Phys. Rev. (in press).

[8]H. Crannell, J. M. Finn, P. Hallowell, J. T. O'Brien, N. Ensslin, L. W. Fagg, E. C. Jones, Jr., and W. L. Bendel, Nucl. Phys. **A278**, 253 (1977); F. Ajzenberg-Selove, *ibid.* **A248**, 1 (1975); **A320**, 1 (1979); **A449**, 1 (1986).

[9]I. Talmi (private communication); Phys. Rev. C **39**, 284 (1989).

[10]J. Raynal, program DWBA82, CEN-Saclay (unpublished).

[11]H. V. Geramb and K. Nakano in *The Interaction between Medium Energy Nucleons in Nuclei, Bloomington, 1982,* Proceedings of the Workshop on the Interactions Between Medium Energy Nucleons in Nuclei, AIP Conf. Proc. No. 97, edited by Hans-Otto Meyer (AIP, New York, 1983), p. 44; L. Rikus, K. Nakano, and H. V. Geramb, Nucl. Phys. **A414**, 413 (1984).

[12]J. R. Comfort, S. M. Austin, P. T. Debevec, G. A. Moake, R. W. Finlay, and W. G. Love, Phys. Rev. C **21**, 2147 (1980).

[13]T. N. Taddeucci, J. Rapaport, C. C. Foster, and J. R. Comfort, Phys. Rev. C **28**, 969 (1983); T. N. Taddeucci, R. R. Doering, A. Galonsky, and S. M. Austin, *ibid.* **29**, 764 (1984).

[14]J. Rapaport, D. Wang J. A. Carr, F. Petrovich, C. C. Foster, C. D. Goodman, C. Gaarde, J. Larsen, C. A. Goulding, T. N. Taddeucci, D. Horen, and E. Sugarbaker, Phys. Rev. C **36**, 500 (1987).

[15]W. G. Love and M. A. Franey, Phys. Rev. C **24**, 1073 (1981).

[16]W. G. Love, K. Nakayama, and M. A. Franey, Phys. Rev. Lett. **59**, 1401 (1987).

[17]L. Berge, Ph.D. thesis, University of Melbourne, 1988.